IEEE Access
Multidisciplinary | Rapid Review | Open Access Journal

Received February 27, 2019, accepted March 11, 2019, date of publication March 15, 2019, date of current version April 5, 2019.

Digital Object Identifier 10.1109/ACCESS.2019.2905349

Design, Fabrication and Testing of a 3D Printed FBG Pressure Sensor

CHENGYU HONG[1], YIFAN ZHANG[2], AND LALIT BORANA[3]

[1]College of Civil Engineering, Shenzhen University, Shenzhen 518060, China
[2]Engineering Research Center of Technical Textiles, Ministry of Education, Donghua University, Shanghai 201620, China
[3]Department of Civil Engineering, IIT Indore, Indore 453552, India

Corresponding author: Yifan Zhang (zhangyifan@dhu.edu.cn)

This work was supported by the Natural Science Foundation of China (NSFC) under Project 41602352.

ABSTRACT In this paper, a fiber Bragg grating (FBG) pressure sensor was designed and fabricated using 3D printing method for the measurement of vertical pressure. The raw material used for the fabrication of this new pressure sensor was Polylactic Acid (PLA). The effectiveness of embedding FBG sensors inside printed PLA material was first examined taking into account different infill densities. It is found that the FBG sensor can be successfully embedded into PLA material without sacrificing its sensing performance. The change of infill density has no influence on both peak and residual wavelength change of FBG sensors during and after the printing process. All FBG sensors printed inside PLA prototype with different infill density values exhibit almost the same peak and residual wavelength rise values in the printing process. In addition, the higher the density value, the longer the time required to finish printing process. A simple FBG pressure sensor was designed and fabricated according to the successful experience of embedding FBG sensors into printed PLA. Measurement performance of this FBG pressure sensor was examined in laboratory cyclic loading tests. Calibration tests indicate that the maximum measured vertical pressure of this new pressure sensor was 2000 kPa with a measurement sensitivity of 13.22 kPa/pm.

INDEX TERMS Fiber Bragg grating, 3D printing, polylactic acid, vertical pressure, encapsulation method.

I. INTRODUCTION

Fiber Bragg grating (FBG) sensor and the associated devices/systems have been widely applied for structural health monitoring due to its attracting advantages such as multiplexing capability, small size, ease of encapsulation, high sensitivity, light weight, and immunity to Electromagnetic Interference (EMI) [1]–[4]. Pressure is one of the most critical physical parameters in structural health monitoring field. Unfortunately, most of traditional pressure sensors were fabricated based on electrical train gauges, vibration wires, etc. These traditional sensors failed to adapt to harsh field environments such as high humidity and serious electromagnetic interference [5]. In particular, conventional sensors are difficult to implement multipoint distributed pressure monitoring, remote sensing and long-term monitoring over a long distance [6]–[11]. Therefore, design and fabrication of new optical based pressure sensors is a critical research area.

FBG sensing technology as an optical fiber passive sensing system has been widely applied for structural health monitoring and geotechnical monitoring. The FBG is a particular sensing element which can be used to measure strain, stress, temperature, displacement, and pressure [12]–[15]. Design and fabrication of FBG pressure sensors have drawn increasing amount of attention in different measurement fields. Most FBG pressure sensors appear to be temperature dependent and the internal sensor components are highly sensitive to strain change arise from applied pressure [16]–[18]. Pressure sensing can be achieved using different internal structures such as a long period grating fabricated in a cavity ring-down loop [19], cantilever beam structure embedded with FBGs to sense pressure with measurement sensitivity of 258.25 pm/MPa and range of 0 to 2 MPa [20], a thin walled cylinder encapsulated inside a pressure cell for hydraulic pressure measurement with sensitivity of 69.4 pm/MPa and measurement range of 0 $\sim$ 16 MPa [21], two-core holey fiber structure for sensing both pressure and temperature [22]. All these pressure transducers are characterized by specific internal sensing components and their fabrication relies on

The associate editor coordinating the review of this manuscript and approving it for publication was Sukhdev Roy.

traditional fine processing technology. The process of fabrication is normally time consuming, complicated, and large amount of raw materials may be wasted.

Application of 3D printing method for the design, fabrication and optimization of FBG sensors is very limited. Conventional FBG based sensors normally rely on the use of glue or epoxy resin to fix FBG sensors. The use of glue or epoxy may lead to some serious adhesive problems such as incompatibility with different substrates, excessive adhesive, and bond failures. In comparison with traditional fine processing technology, 3D printing technique characterized by material extrusion additive manufacturing (MEAM) process is a simple method for fabricating various functional prototypes [23]–[27]. Advantages of using MEAM for prototype mold manufacturing include quick prototyping at high precision, time saving, ease of design, etc. Currently 3D printing technique has been proposed for the development of microscale structures of some traditional sensors [28]–[30]. Nevertheless, few studies have been found focusing on the applications of 3D printing to fabricate different functional optical fiber sensors. Past investigations show that FBG sensors can be successfully embedded into 3D printed prototypes since FBGs are small size and flexible [9]. A new FBG pressure transducer was developed by embedding FBG inside 3D printed ABS (acrylonitrile butadiene styrene) sensing components for the measurement of hydrostatic pressure [27]. But the internal structure consists of complicated components and the measurement of large vertical soil pressure appears to be difficult. Most recently, 3D printing has been used for manufacturing tilt sensors for ground movement monitoring [31]. All these investigations indicate that 3D printing can be used for the design and quick fabrication of a wide variety of FBG based sensors in application [32].

In this study, a simple large size FBG pressure sensor was manufactured using 3D printing process. This pressure sensor was mainly fabricated by embedding a bare FBG sensor inside PLA material. In addition to the main advantages of FBG sensors such as multiplexing, light weight, and remote sensing without significant single loss, this FBG pressure sensor is also characterized by the advantages of quick fabrication, ease of customization, and varied measurement sensitivities and ranges according to sensing requirements.

II. DESIGN AND FABRICATION OF FBG PRESSURE SENSOR USING MEAM PROCESS

A. SENSING PRINCIPLE OF FBG SENSOR

FBG sensor is an optical based sensing technology developed for the measurement of external strain, temperature, and stress in terms of wavelength shift of grating period. Measurement mechanism of FBGs is mainly based on the principle of Bragg reflection. Fig.1 depicts a schematic figure of working principle of a FBG sensor. It is seen a broadband light is injected into the fiber core and reflected light and transmitted light are motivated at the grating location due to the light inference effect. The wavelength variation caused by

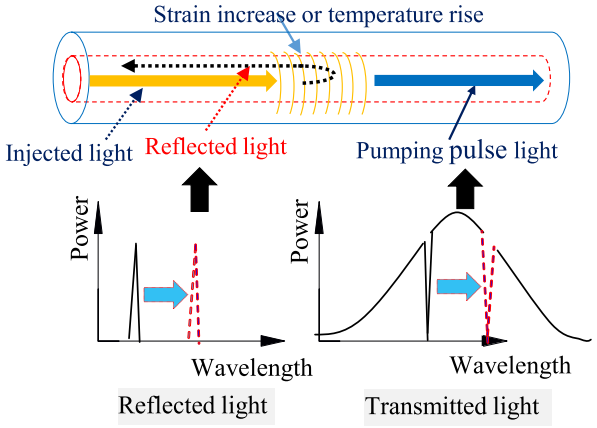

FIGURE 1. Work principle of fiber Bragg grating sensor.

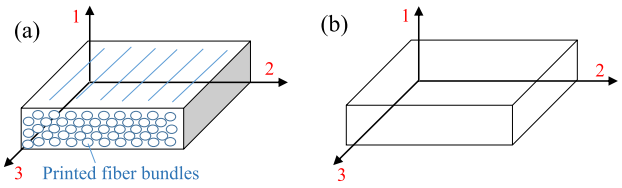

FIGURE 2. Assumed orthotropic 3D printed material; (a) microstructural detail, and (b) continuum model.

axial strain change $\Delta\varepsilon$ and temperature change ΔT can be given by:

$$\frac{\Delta\lambda}{\lambda} = (1 - p_{eff})\Delta\varepsilon + (\alpha + \xi)\Delta T \tag{1}$$

where $\Delta\lambda$, and λ are wavelength change and wavelength value, respectively. p_{eff}, α and ξ are photo-elastic parameter, thermal expansion coefficient and thermal-optic coefficient, respectively. Influence of temperature change should be eliminated to obtain pure strain change of FBG sensors.

B. SENSING MECHANISM OF A FBG PRESSURE SENSOR

A pressure sensor was fabricated using MEAM process with FBG sensors directly embedded into PLA material during printing process inside a 3D printer. The internal FBG is ignored due to the very small size (diameter < 1 mm) compare with the printed PLA prototype ($100 \times 100 \times 10$ mm). Figure 2a show a schematic view of prototype model created by printed PLA fibers. The printed PLA prototype is approximated as an orthotropic material with three orthogonal planes of microstructural symmetry (Figure 2b).

Three material directions including 1, 2, and 3 are also marked in this figure. Considering a pressure sensor element undergoing uniaxial compression, a stiffness matrix with nine independent elastic constants C_{ij}'s can be given by:

$$\begin{bmatrix} \sigma_{11} \\ \sigma_{22} \\ \sigma_{33} \end{bmatrix} = \begin{bmatrix} C_{11} & C_{12} & C_{13} \\ C_{21} & C_{22} & C_{23} \\ C_{31} & C_{32} & C_{33} \end{bmatrix} \begin{bmatrix} \varepsilon_{11} \\ \varepsilon_{22} \\ \varepsilon_{33} \end{bmatrix} \tag{2}$$

where σ_{ii} and ε_{ii} are stress and strain components in three directions, respectively. It is noted that in case the strain is not vertical to the FBG pressure sensor, the stress/strain can also be obtained according to the most general form of Hooke's law. The above relationship can be inverted to the following relationship considering elastic constants E and Poisson's ratio v:

$$\begin{bmatrix} \varepsilon_{11} \\ \varepsilon_{22} \\ \varepsilon_{33} \end{bmatrix} = \begin{bmatrix} \frac{1}{E_1} & -\frac{v_{21}}{E_2} & -\frac{v_{31}}{E_3} \\ -\frac{v_{12}}{E_1} & \frac{1}{E_2} & -\frac{v_{32}}{E_3} \\ -\frac{v_{13}}{E_1} & -\frac{v_{23}}{E_2} & \frac{1}{E_3} \end{bmatrix} \begin{bmatrix} \sigma_{11} \\ \sigma_{22} \\ \sigma_{33} \end{bmatrix} \quad (3)$$

For A pressure sensor subjected to vertical load, $\sigma_{22} = \sigma_{33} = 0$ and $\varepsilon_{22} = \varepsilon_{33}$, we may simply write:

$$\begin{bmatrix} \varepsilon_{11} \\ \varepsilon_{22} \\ \varepsilon_{33} \end{bmatrix} = \begin{bmatrix} \frac{1}{E_1} & -\frac{v_{21}}{E_2} & -\frac{v_{31}}{E_3} \\ -\frac{v_{12}}{E_1} & \frac{1}{E_2} & -\frac{v_{32}}{E_3} \\ -\frac{v_{13}}{E_1} & -\frac{v_{23}}{E_2} & \frac{1}{E_3} \end{bmatrix} \begin{bmatrix} \sigma_{11} \\ 0 \\ 0 \end{bmatrix} \quad (4)$$

where E_i represents the Young's modulus of the printed PLA material in direction $i(i = 1, 2, 3)$; for example, $\sigma_1 = E_1\varepsilon_1$ denotes the stress component for uniaxial tension/compression in direction 1. v_{ij} denotes the Poisson's ratio, representing the ratio of a transverse strain to the occurred strain in uniaxial tension. Eq.(5) can be decomposed into following three relationships:

$$\varepsilon_{11} = \frac{1}{E_1}\sigma_{11}, \quad \varepsilon_{22} = -\frac{v_{21}}{E_2}\sigma_{11}, \quad \varepsilon_{33} = -\frac{v_{13}}{E_1}\sigma_{11} \quad (5)$$

FBG sensor embedded inside the PLA material is subjected to vertical pressure change, which can be quantitatively reflected in terms of wavelength change of FBG sensors. In case there is one FBG sensor embedded into printed PLA material along direction 2, the wavelength change with respect to vertical pressure σ_{11} can be directly obtained considering Eq.(1) and Eq.(5):

$$\Delta\varepsilon_{22} = -\frac{v_{21}}{E_2}\Delta\sigma_{11} = \frac{\Delta\lambda}{(1 - p_{eff})\lambda} - \frac{(\alpha + \xi)\Delta T}{(1 - p_{eff})} \quad (6)$$

Vertical pressure change associated with temperature and wavelength change of FBG pressure sensor can be obtained considering Eq.(6):

$$\Delta\sigma_{11} = \frac{E_2}{v_{21}}\left[\frac{(\alpha + \xi)\Delta T}{(1 - p_{eff})} - \frac{\Delta\lambda}{(1 - p_{eff})\lambda}\right] \quad (7)$$

Eq.(7) is the theoretical equation of using wavelength change to compute vertical pressure above PLA pressure sensor. Eq.(6) and Eq.(7) reveal that the wavelength change $\Delta\lambda$ of a FBG sensor can be used to obtain the vertical pressure $\Delta\sigma_{11}$ occurred above 3D printed PLA prototype.

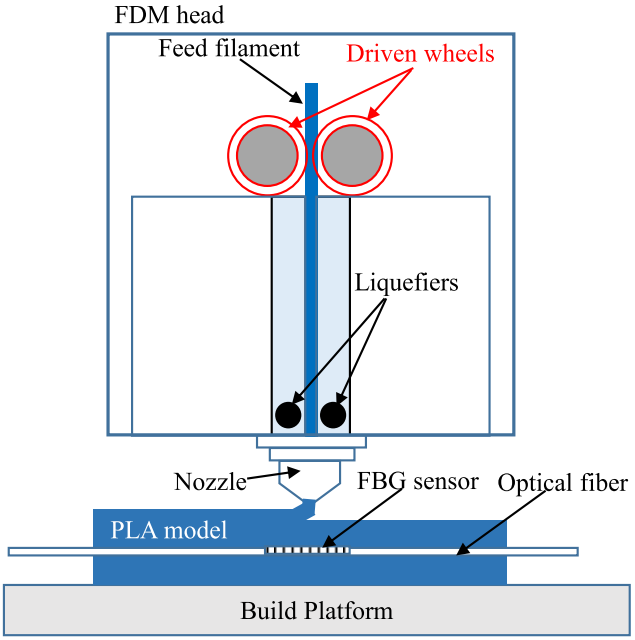

FIGURE 3. A schematic diagram of using MEAM to embed FBG inside fused PLA model.

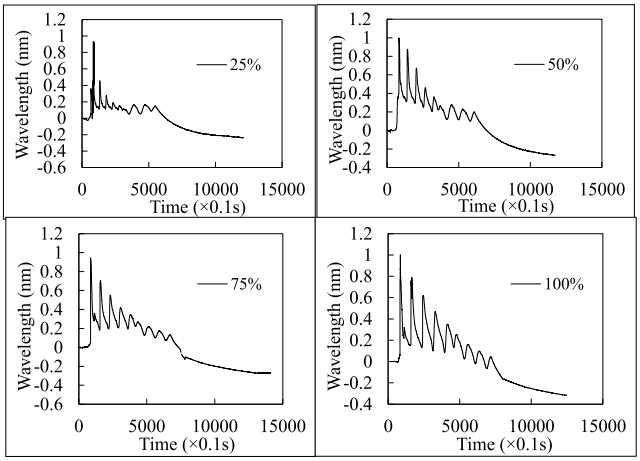

FIGURE 4. Wavelength change of FBG sensors during printing process at printing densities of 25%, 50%, 75%, 80%, and 100%.

C. FABRICATION PROCESS OF A FBG PRESSURE SENSOR USING MEAM PROCESS

MEAM is a technical process for quick fabrication, modeling and prototyping of different products using plastic or wax materials. In this process, raw material is extruded through a nozzle tracing cross sectional geometry of a prototype model layer by layer. A number of materials are available for MEAM such as acrylonitrile butadiene styrene copolymers (ABS), polylactic acid (PLA), polyvinyl chloride (PVC), thermoplastic polyurethanes (TPU), and investment casting wax. Figure 3 depicts a schematic diagram of using MEAM to embed a FBG inside fused PLA model in present study. The 3D printer mainly consists of two driven rollers for feeding filament into two liquefiers, and a nozzle for extruding melted

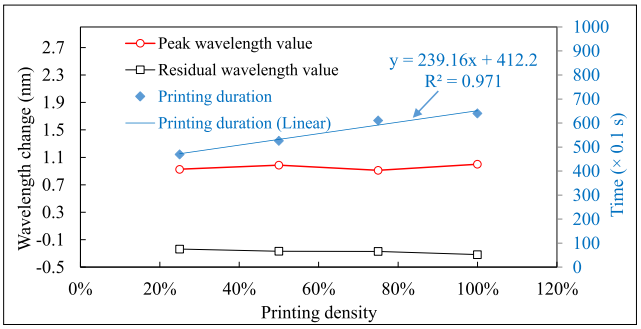

FIGURE 5. Peak and residual wavelength of FBG sensors and printing duration of printing process at different infill density values.

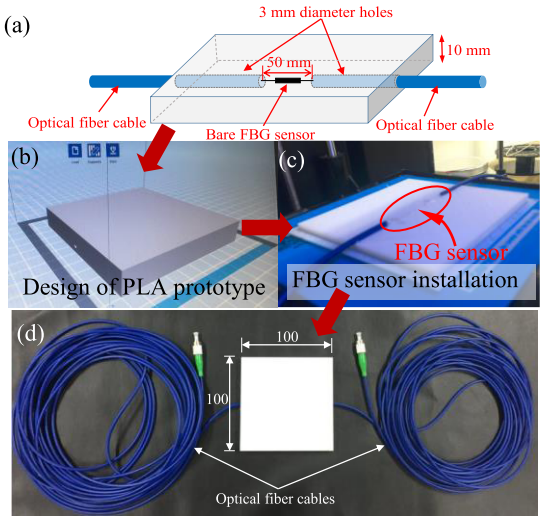

FIGURE 6. (a) A schematic view of FBG pressure sensor, (b) design of PLA prototype, (c) FBG installation, and (d) the FBG pressure sensor after manufacturing. (Unit: mm).

PLA material over the upper surface of a build platform to form the final shape of prototype. The two liquefiers will heat PLA material up to melting point at a temperature 220°C, printing the melted PLA layer by layer. In this study, the interrogator used for FBG data collection is Sm 125 from Micron Optics. The printer brand was Finder (without heated bed) and the selected PLA for the fabrication of pressure sensors was white characterized a diameter of 1.75 mm. Both the printer and flexible PLA were from Flashforge Corporation in mainland China. Motor stepping rate, nozzle size, and printing speed were 5 mm/s, 0.4 mm, and 60 mm/s, respectively.

To verify the feasibility of embedding bare FBG sensors using MEAM process, four different FBG sensors were selected and embedded into PLA material inside a printing machine. The selected four FBG sensors are characterized by initial central wavelength values of 1531.2 nm, 1535.6 nm, 1542.2 nm, and 1551.7 nm, respectively. Length of these FBG sensors was 10 mm. Bandwidth@3dB, side-lobe suppression ratio (SLSR), and reflectivity are $<$0.3 nm, $>$15 dB, and $>$90%, respectively. The infill pattern was hexagon with infill density values varying at 20%, 40%, 60%, 80%, and 100%. Infill density defines the amount of plastic used on the inside of printed materials. Dimension of the printed prototype was 20 mm, 40 mm and 50 mm (height $\times$ width $\times$ length). FBG sensors were directly placed at the upper surface of the printed prototype when 50% size was finished inside the printer. Then the wavelength change of FBG sensors was collected continuously at a frequency of 10 Hz. Figure 4 shows wavelength change of four FBG sensors with different infill densities during printing process. It is clear that priting process was finished within 12 minutes chracterized by a number of peak wavelength values. A total of 9 wavelength peaks are observed for infill densities of 50%, 75%, and 100%, but 8 peak wavelength values are found for infill density of 25%. Existent of these peak wavelength values is due to the significant thermal expansion when the melted PLA material covers the bare FBG sensors during printing. A maximum rise of wavelength value is highly consistent for all four FBG sensors (around 1 nm).

Figure 5 presents the peak/residual wavelength data of FBG sensors and printing duration at different infill density values. Variations of peak and residual wavelength values are highly stable maining at around 1 nm and -0.2 nm, respectively. It is noted that 1 nm wavelength rise of FBG sensor corresponds to a temperature rise of around 100 °C. This reveals that temperature of the melted PLA decreases very quickly after extruded out of the printer nozzle, approaching around 100 °C when covering the FBG sensor section. But a residual wavelength change of around -0.2 nm is finally obtained (at around 1200 seconds), indicating that the PLA material exhibits substantial shrinkage deformation after the PLA material is hardened. Though the whole printing process leads to significant wavelength fluctuation of FBG sensor inside PLA mateiral, but these FBG sensors remain working. Printing duration is found to vary linearly against infill density. The higher the infill density, the shorter the printing duration. This phonomenon indicates that the requried time to finish a printed prototype with relatively higher density is longer.

Figure 6 presents the FBG pressure sensor fabricated using MEAM process in this study. The proposed pressure sensor was cubic shape with one FBG sensor placed in the middle position for strain measurement (Fig.6a). This PLA prototype was first designed using CATIA (Fig.6b). A single FBG sensor was embedded into PLA when 50% size of the pressure sensor was printed, and the printing process has to cease for 1-2 minutes for the placement and fixation of FBG sensor inside PLA prototype (Fig.6c). Grating length of the FBG is 10 mm, and armored fiber optic cable was used to protect two ends of the FBG sensor. The final FBG pressure sensor was characterized by a dimension of 100 mm long, 100 mm wide, and 10 mm high (Fig.6d). Fabrication process of a FBG pressure sensor was finished within 50 minutes. The selected infill density and infill pattern of PLA material were 80% and line shape, respectively. No glue was used to adhere FBG sensor inside printed PLA.

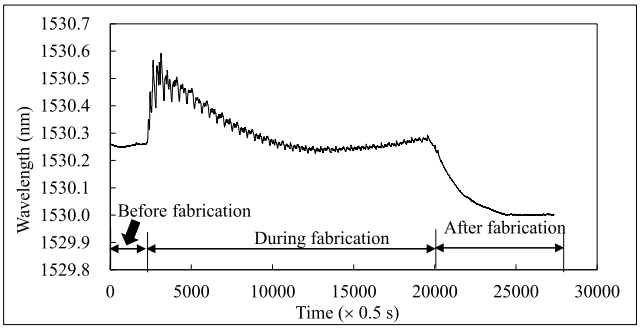

FIGURE 7. Wavelength variation against time during fabrication process of a FBG pressure sensor inside a 3D printer.

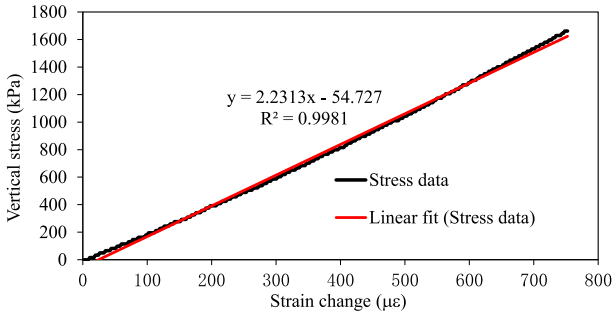

FIGURE 8. Relationship of applied stress against strain change of the FBG pressure sensor.

D. WAVELENGTH VARIATION OF A FBG DURING PRINTING PROCESS

The reflected wavelength change of FBG sensor during MEAM process was collected by an interrogator at a frequency of 10 Hz immediately after FBG sensor was placed inside PLA prototype. The selected infill density was 80%. Figure 7 describes the change of FBG sensor wavelength before, during and after fabrication of pressure sensor. Three typical wavelength phases characterized by different wavelength variation trends can be clearly observed. The wavelength change before printing started is stable, presenting at around 1530.25 nm. Then the wavelength increases quickly approaching about 1530.58 nm at 1250 seconds. Wavelength change of the FBG sensor between 1250 and 10000 seconds exhibits significant initial wavelength fluctuation due to the interaction between FBG sensor and melted PLA material. Each small cycle of wavelength rise and decrease is a reflection of the melted PLA extruded from the printer nozzle covering and detaching the FBG section. FBG wavelength remains decrease for 2000 seconds and finally stabilized at 1530 nm. This substantial wavelength reduction (around 209 $\mu\varepsilon$) is due to the thermal contraction of PLA material during hardening process.

III. CALIBRATION TEST

FBG pressure sensor fabricated using MEAM process was calibrated in a laboratory where room temperature was stable. Vertical pressure was first continuously applied on the top of the FBG pressure sensor to examine the occurred vertical strain change. Figure 8 shows relationship of the applied stress against strain change of the FBG pressure sensor in vertical direction. This linear stress strain relationship can be used to calculate the elastic modulus of the fabricated FBG pressure sensor in vertical direction (around 2.23 GPa).

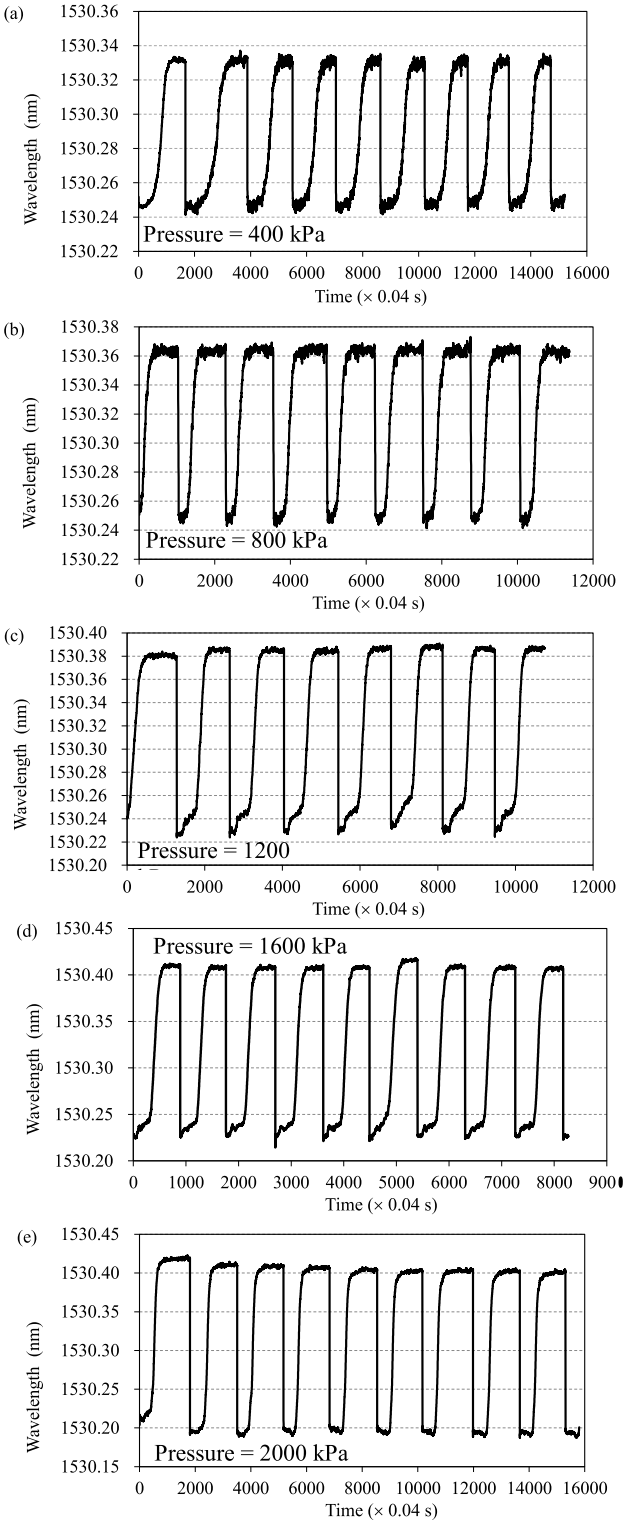

FIGURE 9. Measured wavelength variations against elapsed time in calibration tests for vertical pressures varying at (a) 400 kPa, (b) 800 kPa, (c) 1200 kPa, (d) 1600 kPa, and (e) 2000 kPa.

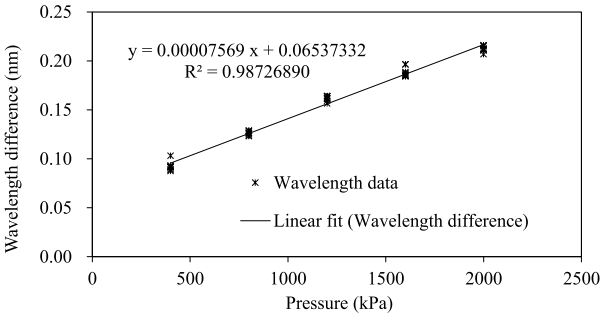

FIGURE 10. Wavelength difference against vertical pressure of FBG pressure sensor.

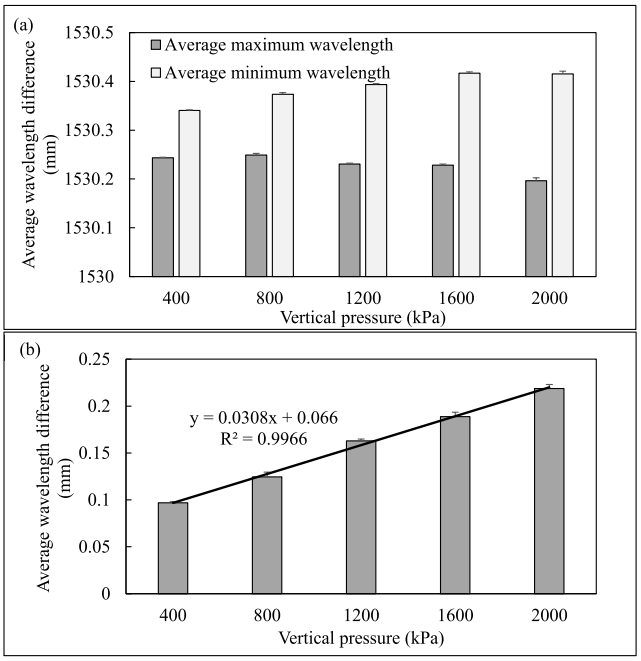

FIGURE 11. (a) Relationships between average maximum and minimum wavelength and vertical pressures and (b) relationships between average wavelength difference and vertical pressures.

Pressure calibration test was carried out by applying vertical pressures varying at 400 kPa, 800 kPa, 1200 kPa, 1600 kPa, and 2000 kPa, respectively. All vertical pressures were totally released after maintaining for around 30-40 seconds in each cycle. A total of 9 loading cycles were conducted for each loading level. Figure 9 presents FBG wavelength variations versus time at different pressure levels. It is clear that the FBG sensor exhibits consistent cyclic wavelength change at five different loading levels. The recorded maximum and minimum wavelength values in each loading cycle are mostly consistent. This indicates that the measurement performance of FBG pressure sensor are stable under cyclic loading tests.

To quantitatively analyze the FBG performance under different vertical pressures, wavelength difference arise from different vertical load in each loading test is summarized in Figure 10. A clear linear relationship of wavelength difference against vertical pressure is obtained. The slope ratio can be used to compute the magnitudes of vertical pressure applied on the top of pressure sensor in terms of wavelength change of FBG inside the pressure sensor.

All the maximum and minimum wavelength values and the related standard deviations are summarized in Figure 11a to investigate the amount of wavelength dispersion. The maximum and minimum standard deviations of maximum and minimum wavelength values are 0.0068 nm and 0.0057 nm, respectively. Figure 11b shows the relationship of average wavelength difference change against vertical pressure. It is also clear from the fitted linear relationship that the average wavelength difference increases linearly as the increase of vertical pressure. The obtained maximum standard deviation is also very limited (0.005 nm), indicating that the relative wavelength variation with respect to mean wavelength difference is ignorable.

IV. CONCLUSIONS

In this study, a 3D printed FBG pressure sensor was designed and fabricated using material extrusion additive manufacturing (MEAM) method. Mechanical performance of the printed FBG pressure sensor was examined in laboratory calibration tests. Conclusions and main findings of this study are drawn as follows:

(a) A new FBG based pressure sensor was successfully fabricated using MEAM process by embedding a bare FBG sensor inside a printed PLA prototype. This fabrication method is characterized by the advantages of quick fabrication and better protection, avoiding the use of glue or epoxy resin during encapsulation process.

(b) Thermal expansion during printing process of PLA material leads to significant wavelength rise of FBG sensors (around 1 nm) after printing started, but with a residual wavelength of -0.2 nm after printed material is hardened. Changing in infill densities appears have no influence on both peak and residual wavelength values during printing process. The required time to embed a FBG sensor within a lower density is relatively shorter.

(c) The collected pressure sensor data during MEAM process indicates that FBG sensor can be successfully embedded inside fused PLA material. The FBG sensor is subjected substantial contraction (around 209 $\mu\varepsilon$) after MEAM process is completed. Calibration test show that the new FBG pressure sensor presented reliable measurement performance. Wavelength difference of FBG sensor varies linearly against applied vertical pressure in calibration test. Measurement range and sensitivity of FBG pressure sensor are 0-2000 kPa and 13.22 kPa/pm, which can be revised according to test requirement by changing different printing parameters such as infill densities, infill pattern, and raw materials with different stiffness.

Due to the limited budget and time, this study only concerned using PLA to fabricate a FBG pressure sensor at infill density of 80%. The authors will carry out more tests in future focusing on sensor performance fabricated with different infill

densities and infill patterns, as well as different filaments (ABS, PVC, TPU, etc.).

REFERENCES

[1] S. Umesh and S. Asokan, "A brief overview of the recent bio-medical applications of fiber Bragg grating sensors," *J. Indian Inst. Sci.*, vol. 94, no. 3, pp. 319–328, 2014.

[2] Y. Hu, C. Hong, Y. Zhang, and G. Li, "A monitoring and warning system for expressway slopes using FBG sensing technology," *Int. J. Distrib. Sensor Netw.*, vol. 14, no. 5, 2018, Art. no. 1550147718776228.

[3] A. K. Singh, S. Berggren, Y. Zhu, M. Han, and H. Huang, "Simultaneous strain and temperature measurement using a single fiber Bragg grating embedded in a composite laminate," *Smart Mater. Struct.*, vol. 26, no. 11, 2017, Art. no. 115025.

[4] R. Suresh, S. C. Tjin, and N. Q. Ngo, "Application of a new fiber Bragg grating based shear force sensor for monitoring civil structural components," *Smart Mater. Struct.*, vol. 14, no. 5, p. 982, 2005.

[5] J. Huang, Z. Zhou, D. Zhang, and Q. Wei, "A fiber Bragg grating pressure sensor and its application to pipeline leakage detection," *Adv. Mech. Eng.*, vol. 2013, 2013, Art. no. 590451.

[6] C. Y. Hong, J. H. Yin, H. F. Pei, E. M. Xu, and W. H. Zhou, "Study on cement grout quality of model soil nails measured using long gage FBG sensing technology," in *Proc. 17th Southeast Asian Geotechnical Conf.*, Taipei, Taiwan, 2010, pp. 237–240.

[7] C. Y. Hong, Y. F. Zhang, M. X. Zhang, L. M. G. Leung, and L. Q. Liu, "Application of FBG sensors for geotechnical health monitoring, a review of sensor design, implementation methods and packaging techniques," *Sens. Actuators A, Phys.*, vol. 244, pp. 184–197, May 2016.

[8] A. Kantaros and D. Karalekas, "Fiber Bragg grating based investigation of residual strains in ABS parts fabricated by fused deposition modeling process," *Mater. Des.*, vol. 50, pp. 44–50, Sep. 2013.

[9] P. Liacouras, G. Grant, K. Choudhry, G. F. Strouse, and Z. Ahmed. (2015). "Fiber Bragg gratings embedded in 3D-printed scaffolds." [Online]. Available: https://arxiv.org/abs/1508.01156

[10] C. Shen and C. Zhong, "Novel temperature-insensitive fiber Bragg grating sensor for displacement measurement," *Sens. Actuators A, Phys.*, vol. 170, no. 1, pp. 51–54, 2011.

[11] G. Tang *et al.*, "A fiber Bragg grating based tilt sensor suitable for constant temperature room," *J. Opt.*, vol. 17, no. 7, 2015, Art. no. 075701.

[12] S. C. Kang, S. Y. Kim, S. B. Lee, S. W. Kwon, S. S. Choi, and B. Lee, "Temperature-independent strain sensor system using a tilted fiber Bragg grating demodulator," *IEEE Photon. Technol. Lett.*, vol. 10, no. 10, pp. 1461–1463, Oct. 1998.

[13] F. Li, W. T. Zhang, F. Li, and Y. L. Du, "Fiber optic inclinometer for landslide monitoring," *Appl. Mech. Mater.*, vols. 166–169, pp. 2623–2626, May 2012.

[14] B.-O. Guan, H.-Y. Tam, and S.-Y. Liu, "Temperature-independent fiber Bragg grating tilt sensor," *IEEE Photon. Technol. Lett.*, vol. 16, no. 1, pp. 224–226, Jan. 2004.

[15] R.-S. Shen *et al.*, "Study on high-temperature and high-pressure measurement by using metal-coated FBG," *Microw. Opt. Technol. Lett.*, vol. 50, no. 5, pp. 1138–1140, 2008.

[16] A.-B. Huang, K.-W. Wu, M. Z. E. B. Elshafie, W.-Y. Hung, and Y.-T. Ho, "Development of an FBG-sensed miniature pressure transducer and its applications to geotechnical centrifuge modelling," in *Proc. China-Eur. Conf. Geotechnical Eng.* Amsterdam, The Netherlands: Springer, 2018, pp. 694–698.

[17] Z. Zhou and J. Ou, "Development of FBG sensors for structural health monitoring in civil infrastructures," in *Sensing Issues in Civil Structural Health Monitoring*. Cham, Switzerland: Springer, 2005, pp. 197–207.

[18] T. S. Mansour and F. M. Abdulhussein, "Dual measurements of pressure and temperature with fiber Bragg grating sensor," *Al-Khwarizmi Eng. J.*, vol. 11, no. 2, pp. 86–91, 2015.

[19] N. Ni, C. C. Chan, W. C. Wong, L. Y. Shao, X. Y. Dong, and P. Shum, "Cavity ring-down long period grating pressure sensor," *Sens. Actuators A, Phys.*, vol. 158, no. 2, pp. 207–211, 2010.

[20] Y. Zhao, H.-K. Zheng, R.-Q. Lv, and Y. Yang, "A practical FBG pressure sensor based on diaphragm-cantilever," *Sens. Actuators A, Phys.*, vol. 279, pp. 101–106, Aug. 2018.

[21] Y.-F. Gu, Y. Zhao, R.-Q. Lv, and Y. Yang, "A practical FBG sensor based on a thin-walled cylinder for hydraulic pressure measurement," *IEEE Photon. Technol. Lett.*, vol. 28, no. 22, pp. 2569–2572, Nov. 15, 2016.

[22] L. Htein, Z. Liu, B. Zhou, and H.-Y. Tam, "Bragg grating in novel two-core holey fiber for simultaneous measurement of pressure and temperature," in *Proc. Opto-Electron. Commun. Conf. (OECC) Photon. Global Conf. (PGC)*, Jul./Aug. 2017, pp. 1–2.

[23] Z. Zhou *et al.*, "Optical fiber Bragg grating sensor assembly for 3D strain monitoring and its case study in highway pavement," *Mech. Syst. Signal Process.*, vol. 28, pp. 36–49, Apr. 2012.

[24] K. Willis, E. Brockmeyer, S. Hudson, and I. Poupyrev, "Printed optics: 3D printing of embedded optical elements for interactive devices," in *Proc. 25th Annu. ACM Symp. User Interface Softw. Technol.*, 2012, pp. 589–598.

[25] M. G. Zubel, K. Sugden, D. Saez-Rodriguez, K. Nielsen, and O. Bang, "3D printed sensing patches with embedded polymer optical fibre Bragg gratings," in *Proc. 6th Eur. Workshop Opt. Fibre Sensors (EWOFS), Int. Soc. Opt. Photon.*, 2016, Art. no. 99162E.

[26] Y.-F. Zhang, C.-Y. Hong, R. Ahmed, and Z. Ahmed, "A fiber Bragg grating based sensing platform fabricated by fused deposition modeling process for plantar pressure measurement," *Measurement*, vol. 112, pp. 74–79, Dec. 2017.

[27] Y. K. Lin, T. S. Hsieh, L. Tsai, S. H. Wang, and C. C. Chiang, "Using three-dimensional printing technology to produce a novel optical fiber Bragg grating pressure sensor," *Sensors Mater*, vol. 28, no. 5, pp. 389–394, 2016.

[28] T. M. Llewellyn-Jones, B. W. Drinkwater, and R. S. Trask, "3D printed components with ultrasonically arranged microscale structure," *Smart Mater. Struct.*, vol. 25, no. 2, 2016, Art. no. 02LT01.

[29] D. Espalin, D. W. Muse, E. MacDonald, and R. B. Wicker, "3D printing multifunctionality: Structures with electronics," *Int. J. Adv. Manuf. Technol.*, vol. 72, nos. 5–8, pp. 963–978, 2014.

[30] S. B. Kesner and R. D. Howe, "Design principles for rapid prototyping forces sensors using 3-D printing," *IEEE/ASME Trans. Mechatronics*, vol. 16, no. 5, pp. 866–870, Oct. 2011.

[31] C. Y. Hong, Y. Zhang, and Z. A. Abro, "A fiber Bragg grating–based inclinometer fabricated using 3-D printing method for slope monitoring," *Geotechnical Test. J.*, vol. 43, no. 1, 2019, Art. no. GTJ20170277.

[32] *Standard Terminology for Additive Manufacturing Technologies*, Standard ASTM F2792-12a, West Conshohocken, PA, USA, 2012.

CHENGYU HONG was born in Harbin, Heilongjiang, China, in 1982. He received the Ph.D. degree in geotechnical engineering from The Hong Kong Polytechnic University, Hong Kong, in 2011. He has developed a number of different optical fiber sensor-based sensors, which have been successfully applied in various research fields during Ph.D. studies. He is currently an Assistant Professor with the College of Civil Engineering, Shenzhen University, focusing on the development of new optical fiber sensors and their applications. His research interest includes the application of different optical fiber sensor technologies in geotechnical engineering. He is currently a reviewer for more than 30 SCI journals.

YIFAN ZHANG was born in Luoyang, Henan, China, in 1983. She received the Ph.D. degree from the Institute of Textiles and Clothing, The Hong Kong Polytechnic University, Hong Kong, in 2013. She joined the Knitting and Clothing Department, College of Textiles, Donghua University, Shanghai, China. Her research interests include the development of smart sensors for textile monitoring and digital textile engineering.

LALIT BORANA was a Postdoctoral Research Fellow with the Department of Civil and Environmental Engineering, Faculty of Construction and Environment, The Hong Kong Polytechnic University, Hong Kong. He is currently an Assistant Professor with the Department of Civil Engineering, IIT Indore, India.